









## Analyzing Energy and Mass Transport in MHD Convective Flow with Variable Suction and Hall Effects on a Vertical Porous Surface

Aruna Ganjikunta<sup>1</sup>, Obulesu Mopuri<sup>2</sup>, Charankumar Ganteda<sup>3</sup>, Vijayalakshmi Arumugam<sup>4</sup>,  
S. Vijayakumar Varma<sup>5</sup>, Vuyyuru Lalitha<sup>6</sup>, Giulio Lorenzini<sup>7\*</sup>

<sup>1</sup> Department of Mathematics, GITAM University, Hyderabad 502329, India

<sup>2</sup> Department of Mathematics, Ramireddy Subbarami Reddy Engineering College (Autonomous), Kadanuthala 524142, India

<sup>3</sup> Department of Mathematics, Koneru Lakshmaiah Education Foundation (KLEF), Vaddeswaram 522302, India

<sup>4</sup> Department of Mathematics, Grt Institute of Engineering and Technology, Tiruttani 631209, India

<sup>5</sup> Department of Mathematics, School of Applied Sciences, REVA University, Bengaluru 560064, India

<sup>6</sup> Department of Computer Science & Engineering, Koneru Lakshmaiah Education Foundation (KLEF), Vaddeswaram 522302, India

<sup>7</sup> Department of Industrial Systems and Technologies Engineering, University of Parma, Parma 43124, Italy

Corresponding Author Email: [giulio.lorenzini@unipr.it](mailto:giulio.lorenzini@unipr.it)

Copyright: ©2024 The authors. This article is published by IETA and is licensed under the CC BY 4.0 license (<http://creativecommons.org/licenses/by/4.0/>).

<https://doi.org/10.18280/ijcmem.120402>

### ABSTRACT

**Received:** 9 October 2024

**Revised:** 28 November 2024

**Accepted:** 17 December 2024

**Available online:** 27 December 2024

#### Keywords:

*MHD, heat absorption, thermal radiation, radiation absorption, DuFour effect, Hall effect*

The chemical response and the collective buoyancy effects of thermal and mass diffusion in magnetohydrodynamic (MHD) convection are analyzed on an infinite vertical surface with porous material that emits gas as it rises. This study investigates how the governing equations perform under a broad range of stringent conditions, incorporating subjective considerations such as determining which factor dominates—suction velocity or Hall current strength. Ancillary currents were also considered to provide a comprehensive analysis. The governing equations for liquid flow were solved using the perturbation technique, yielding results in terms of temperature, concentration, and velocity fields. Dimensionless profiles of temperature, velocity, and concentration are graphically presented for various parameter values. It is observed that an increase in the Dufour number leads to higher primary and secondary velocities, as well as increased temperature. Conversely, primary and secondary velocities decrease with an increase in the chemical reaction number and magnetic field strength.

## 1. INTRODUCTION

Today a lot of experts are focusing on the qualities of how liquids move. Beneficial for many different uses in technology and healthcare. "And more attention will be given to how it works in different types of liquid flows." Some of these functions are used in the fields of Metrology and Solar Physics. Later on, many different industries have experienced growth and success in MHD flow. Kumar et al. [1] discussed their insights regarding unstable MHD with the potential impact of the Hall effect on a vertical plate that can move instantaneously along with other effects. Kumaresan and Kumar [2] conducted a study to review Walter's liquid-B model for magnetic fluid flow on a plate, including the effects of species diffusion and uniform temperature. Jain and Choudhary [3] thoroughly studied how heat and magnetic fields affect the flow of particles in Thermophoretic MHD Flow, examining the roles of Soret and Dufour effects in temperature transport and also considering chemical reactions on a non-linear expanding surface. Gangadhar et al. [4] provided a brief discussion about MHD nanofluid flow with Newtonian heating via a stretchable sheet. Chu et al. [5]

discussed hybrid nanofluids MHD flow via a sloping platform with a porous medium. Prabhakar Reddy and Sademaki [6] studied the flow of MHD Casson liquid with Newtonian heating through a porous plate that moves up and down.

Magnetohydrodynamics, which involves heat absorption, has caught the attention of engineers and academics due to its applications in various fluid flows in both nature and industry. Kabir and Al Mahbub [7] provided a theoretical explanation of how the movement of particles due to heat affects the flow of a fluid with heat generation when a magnetic field is applied. Sinha and Mahanta [8] conducted parametric research on MHD unsteady flow with mass and heat transport. Gangadhar et al. [9] discussed dual solutions in Casson fluid flow. Subhakar et al. [10] examined heat production in MHD flow in a stationary ambient fluid on a movable non-isothermal plate in a vertical position. Sandhya et al. [11] explained constant MHD flow with emission and the impact of a temperature gradient on a permeable medium. Das et al. [12] attempted to study how Casson fluid reacts to factors like chemical reactions, heat absorption, and thermal radiation emission. Nihaal et al. [13] briefly demonstrated the presence of thermal emission in a type of liquid called MHD

viscoelastic fluid, which also includes the concentration of different substances.

Several investigators have focused on the effects of chemical reactions and radiation in fluids. Chemical reactions can be replicated as two different processes: homogeneous or heterogeneous, based on phases. In the homogeneous reaction, species generation is identical to its internal source of heat generation. Choudhury and Ahmed [14] addressed the issue with analytical research on MHD convective flow using a vertical plate with a chemical reaction and heat sink, as well as a consistent attractive field placed transversely on the same plate. Choudhury and Das [15] deliberated their viewpoints regarding the utilization of suction velocity via chemical reaction to a vertical porous plate in a viscoelastic flow with MHD. The studies [16-18] provided a clear depiction of MHD through fluids by coupling momentum, energy, and mass with one another using the diffusion equation. Khan et al. [19] were motivated to study the effects of chemical reactions on MHD Micropolar liquid considering double stratification.

The Dufour effect occurs when there is a flow of heat caused by a difference in chemical potential. Extensive studies have been conducted on this gas phenomenon. However, due to the small impact it has, accurate measurements of the Dufour effect in liquids have only been conducted recently. Dagana and Amos [20] aimed to present some discoveries about MHD free flow with the Dufour effect and the effects of chemical reactions. The research of Podder and Samad [21] has been expanded to investigate how the Dufour effect affects a non-Newtonian fluid on a constantly affecting sheet with a consistent exterior heat source. Srinivasacharya and Reddy [22] shared an inspiring piece about mixed convection with the Dufour effect and varying wall temperature in a power-law fluid. Jah and Sarki [23] thoroughly deliberated how the Dufour effects impact the flow of fluid on a porous plate. Some of the related studies to the present investigation are pragmatic in the studies [24-29].

Hall effect sensing is now used in industries to control hydraulic valves. Instead of traditional mechanical levers, Hall effect joysticks are being used for contactless sensing. Different types of vehicles such as mining trucks, backhoe loaders, cranes, diggers, and scissor lifts utilize this technology for various tasks. Recently, the Hall effect has become crucial in determining how the Hall parameter affects entropy generation and electrical conductivity. VeeraKrishna et al. [30] studied how Hall effects impact the movement of a second-grade fluid between two vertical plates. The flow was unsteady and possessed magnetic properties, with the fluid moving due to natural forces and a porous material present between the plates.

Obulesu et al. [31] researched the impact of Hall current on the flow of liquid metal past a porous surface, examining how thermal radiation, chemical reactions, and heat production or absorption influenced the flow. VeeraKrishna and Chamkha [32] investigated how Hall effects affect the flow of a second-grade fluid through a porous medium with varying wall temperature and external concentration. Researchers, including Khlaf et al. [33], have studied how the Hall effect influences flow when various physical factors are present. The scholarly discourse conducted by the studies [34-41], delved into the intricate phenomenon of the Hall effect on MHD flow, elucidating its manifold applications within the realm of fluid dynamics.

The studies mentioned did not take into account the Dufour effect and radiation absorption when Hall currents, chemical

reactions, and heat sources/sinks were present. This paper aims to discuss the Dufour effect and radiation absorption in the presence of Hall currents, chemical reactions, and heat sources/sinks. This paper is a continuation of the work of Obulesu and Prasad [37], considering how the flow of liquid metal is affected by Hall currents as it passes through a porous plate, including factors like thermal radiation, chemical reactions, heat generation/absorption, radiation absorption, and the Dufour effect.

## 2. FORMULATION OF THE PROBLEM

Figure 1 shows the movement of a fluid that conducts electricity over a vertical plate that never ends. This plate can absorb heat and has different levels of suction. In this study we also looked at the Dufour effect and how radiation is absorbed. The horizontal line on the plate is called the x-axis while the vertical line is called the y-axis.

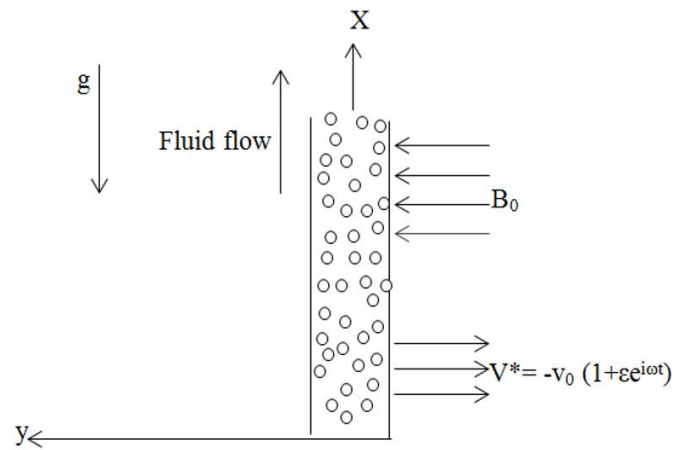


Figure 1. Schematic diagram of the physical model

We will focus on these conditions during our investigation.

- The magnetic field that is created can be ignored because the magnetic field applied sideways and the attractive Reynolds number are very low for metal liquids and partly ionized fluids. There is no electric meadow because no voltage is applied. The Hall effect is studied to understand how strong the magnetic field is.

- The fluid's temperature is controlled by an energy equation that includes radiative heat flow heat source/sink the Dufour effect radiation absorption and a species concentration equation that involves a first-order substance response.

According to Boussinesq's approximation and boundary layer theory the equations that control the issue we are looking at are:

Continuity equation:

$$\frac{\partial V^*}{\partial y^*} = 0 \quad (1)$$

Momentum equation:

$$\frac{\partial u^*}{\partial t^*} + V^* \frac{\partial u^*}{\partial y^*} = \frac{\partial U^*}{\partial t^*} + \nu \frac{\partial^2 u^*}{\partial y^{*2}} + g\beta(T^* - T_\infty) + gB(C^* - C_\infty) - \frac{\sigma B_0^2}{\rho(1 + m^2)}(u^* - U + mw) - \frac{\vartheta}{K}(u^* - U) \quad (2)$$

$$\begin{aligned} \frac{\partial w^*}{\partial t^*} + V^* \frac{\partial w^*}{\partial y^*} &= \vartheta \partial^2 \frac{w^*}{\partial y^{*2}} \\ + \frac{\sigma B_0^2}{\rho(1+m^2)} [m(u^* - U) - w] - \frac{\vartheta}{K} w \end{aligned} \quad (3)$$

Energy equation:

$$\begin{aligned} \frac{\partial T^*}{\partial t^*} + V^* \frac{\partial T^*}{\partial y^*} &= \frac{K}{\rho C_p} \partial^2 \frac{T^*}{\partial y^{*2}} - \frac{1}{\rho C_p} \frac{\partial q_r^*}{\partial y^*} \\ - \frac{Q}{\rho C_p} (T^* - T_\infty) + \frac{Q_1}{\rho C_p} (C^* - C_\infty) + \frac{D_m}{\rho C_p} \partial^2 \frac{C^*}{\partial y^{*2}} \end{aligned} \quad (4)$$

Concentration equation:

$$\frac{\partial C^*}{\partial t^*} + V^* \frac{\partial C^*}{\partial y^*} = D \partial^2 \frac{C^*}{\partial y^{*2}} - K_c (C^* - C_\infty) \quad (5)$$

The appropriate border line circumstances are given as follows:

$$\begin{aligned} u^* = 0, w^* = 0, T^* = T_w, C^* = C_w \text{ at } y = 0 \\ u^* \rightarrow U(t), w^* \rightarrow 0, T^* \rightarrow T_\infty, C^* \rightarrow C_\infty \text{ as } y \rightarrow \infty \end{aligned} \quad (6)$$

The plate is subjected to a time-dependent variable suction velocity, allowing us to replace  $V = -v_0 (1 + \varepsilon e^{i\omega t})$  ( $\varepsilon \ll 1$ ). Where  $v_0$  is the steady suction velocity.

When we talk about non-dimensional quantities, we are referring to specific measurements that do not have any units.

$$\begin{aligned} u &= \frac{u^*}{U_0}, w = \frac{w^*}{U_0} y = v_0 \frac{y^*}{\vartheta}, t = \frac{t^* v_0^2}{4\vartheta} \\ T &= \frac{T^* - T_\infty}{T_w - T_\infty}, \lambda = \frac{C^* - C_\infty}{C_w - C_\infty}, Pr = \frac{\mu C_p}{K}, \\ zSc &= \frac{\vartheta}{D}, M^2 = \frac{\sigma B_0^2 \vartheta}{\rho v_0^2}, Gr = \frac{\vartheta g \beta (T_w - T_\infty)}{U_0 v_0^2}, \\ Gm &= \frac{\vartheta g \beta (C_w - C_\infty)}{U_0 v_0^2}, K_1 = \frac{K v_0^2}{\vartheta^2}, U = \frac{U^*}{U_0}, \\ Kr &= \frac{\vartheta K_c}{v_0^2}, R = \frac{16\sigma T_\infty^3}{3\kappa\kappa}, Q = \frac{Q v^2}{K v_0^2}, \\ Ra &= \frac{Q_1 v^2 (C_w - C_\infty)}{K v_0^2 (T_w - T_\infty)}, Du = \frac{D_m (C_w - C_\infty)}{K (T_w - T_\infty)} \end{aligned} \quad (7)$$

We attain the subsequent equations in dimensionless appearance.

$$\begin{aligned} \frac{1}{4} \frac{\partial F}{\partial t} - (1 + \varepsilon e^{i\omega t}) \frac{\partial F}{\partial y} - \frac{\partial^2 F}{\partial y^2} \\ + \frac{M^2}{1+m^2} (F - U)(1 - im) = \frac{1}{4} \frac{\partial U}{\partial t} \\ + Gr T + Gm \lambda - \frac{(F - U)}{K_1} \end{aligned} \quad (8)$$

$$\begin{aligned} \frac{Pr}{4} \frac{\partial T}{\partial t} - Pr(1 + \varepsilon e^{i\omega t}) \frac{\partial T}{\partial y} \\ = (1 + R) \frac{\partial^2 T}{\partial y^2} - Q T + R_a \lambda + Du \frac{\partial^2 \lambda}{\partial y^2} \end{aligned} \quad (9)$$

$$\frac{Sc}{4} \frac{\partial \lambda}{\partial t} - Sc(1 + \varepsilon e^{i\omega t}) \frac{\partial \lambda}{\partial y} = \frac{\partial^2 \lambda}{\partial y^2} - Sc Kr \lambda \quad (10)$$

where,  $F = u + iw$ .

The equivalent border line environment is

$$\begin{aligned} F = 0, T = 1, \lambda = 1 \text{ at } y = 0 \\ F = V(t), T \rightarrow 0, \lambda \rightarrow 0 \text{ as } y \rightarrow \infty \end{aligned} \quad (11)$$

### 3. METHOD OF SOLUTION

To explain the curved Eqs. (8) to (10) with the given limits (11), we make the assumption that.

$$\begin{aligned} F = (1 - F_0) + \varepsilon(1 - F_1)e^{i\omega t}, U = 1 + \varepsilon e^{i\omega t}, T \\ = T_0 + \varepsilon T_1 e^{i\omega t}, \lambda = \lambda_0 + \varepsilon \lambda_1 e^{i\omega t} \end{aligned} \quad (12)$$

We will now substitute Eq. (8) with Eq. (10) and compare similar terms ignoring terms  $\varepsilon$  with higher orders, we obtain:

Zero order terms:

$$F_0'' + F_0' - (\alpha_1 + \frac{1}{K_1})F_0 = GrT_0 + Gm\lambda_0 \quad (13)$$

$$(1 + R)T_0'' + Pr\{T_0' - QT_0\} = -Du\lambda_0'' - Ra\lambda_0 \quad (14)$$

$$\lambda_0'' + Sc\{\lambda_0' - ScKr\lambda_0\} = 0 \quad (15)$$

First order terms:

$$F_1'' + F_1' - (\alpha_1 + \frac{i\omega}{4} + \frac{1}{K_1})F_1 = -\frac{\partial F_0}{\partial y} + GrT_1 + Gm\lambda_1 \quad (16)$$

$$\begin{aligned} (1 + R)T_1'' + Pr\{T_1' - (Q + \frac{i\omega Pr}{4})T_1\} \\ = -Pr \frac{\partial T_0}{\partial y} - Du \frac{\partial^2 \lambda_1}{\partial y^2} - Ra\lambda_1 \end{aligned} \quad (17)$$

$$\lambda_1'' + Sc\{\lambda_1' - Sc(Kr + \frac{i\omega}{4})\lambda_1\} = -Sc \frac{\partial \lambda_0}{\partial y} \quad (18)$$

The border line circumstances are

$$\begin{aligned} F_0 = 1, F_1 = 1, T_0 = 1, T_1 = 0, \\ \lambda_0 = 1, \lambda_1 = 0 \text{ at } y = 0 \\ F_0 \rightarrow 0, F_1 \rightarrow 0, T_0 \rightarrow 0, T_1 \rightarrow 0 \\ \lambda_0 \rightarrow 0, \lambda_1 \rightarrow 0 \text{ as } y \rightarrow \infty \end{aligned} \quad (19)$$

In Eqs. (13) to (18), the primes show the changes in  $y$ . By solving Eq. (13) through Eq. (18) while considering the border line circumstances in Eq. (19), we find the solution.

$$\lambda_1 = \frac{ScA_1}{a_1} (e^{-A_1 y} - e^{-A_2 y}) \quad (20)$$

$$\lambda_0 = e^{-A_1 y} \quad (21)$$

$$T_0 = l_1 e^{-A_3 y} - l_2 e^{-A_1 y} \quad (22)$$

$$T_1 = l_6 e^{-A_3 y} + l_7 e^{-A_2 y} - l_8 e^{-A_1 y} + l_9 e^{-A_4 y} \quad (23)$$

$$F_0 = l_{12} e^{-A_5 y} + l_{10} e^{-A_3 y} + l_{11} e^{-A_1 y} \quad (24)$$

$$\begin{aligned} F_1 = l_{13} e^{-A_1 y} + l_{14} e^{-A_2 y} + l_{15} e^{-A_3 y} + l_{16} e^{-A_4 y} \\ + l_{17} e^{-A_5 y} + l_{18} e^{-A_6 y} \end{aligned} \quad (25)$$

Substituting Eqs. (20)-(25) in Eq. (12) we obtain the speed, hotness and attentiveness meadow:

$$F = [1 - (l_{12}e^{A_5y} + l_{10}e^{-A_3y} + l_{11}e^{-A_1y})] + \varepsilon[1 - (l_{13}e^{-A_1y} + l_{14}e^{-A_2y} + l_{15}e^{-A_3y} + l_{16}e^{-A_4y} + l_{17}e^{-A_5y} + l_{18}e^{-A_6y})]e^{i\omega t} \quad (26)$$

$$T = l_1e^{-A_3y} - l_2e^{-A_1y} + \varepsilon B_1(l_6e^{-A_3y} + l_7e^{-A_2y} - l_8e^{-A_1y} + l_9e^{-A_4y})e^{i\omega t} \quad (27)$$

$$\lambda = e^{-A_1y} - B_2e^{-A_1y} + \varepsilon \frac{ScA_1}{a_1}(e^{-A_1y} - e^{-A_2y})e^{i\omega t} \quad (28)$$

Skin friction:

$$\tau = \left(\frac{\partial F}{\partial y}\right)_{y=0} = (A_3l_{10} + A_1l_{11} + A_5l_{12}) + \varepsilon(A_1l_{13} + A_2l_{14} + A_3l_{15} + A_4l_{16} + A_5l_{17} + A_6l_{18})e^{i\omega t} \quad (29)$$

Rate of heat transfer:

$$Nu = (-A_3l_1 + A_1l_1) + \varepsilon(-A_3l_6 - A_2l_7 + A_1l_8 + A_4l_9)e^{i\omega t} \quad (30)$$

Rate of mass transfer:

$$Sh = -A_1 + \varepsilon \frac{ScA_1}{a_1}(A_2 - A_1)e^{i\omega t} \quad (31)$$

In Eqs. (29)-(31),  $A_1$  to  $A_6$  are mentioned in Appendix.

## 4. RESULTS AND DISCUSSION

### 4.1 Velocity profiles

From Figures 2 and 3, it is observed that as the magnetic field parameter increases, both the primary and secondary velocity fields decrease. When an oblique magnetic field is applied, it generates a Lorentz force that resists the flow of the fluid, thereby slowing it down.

In Figures 4 and 5, the impact of the Grashof number (Gr) on the primary and secondary velocity profiles is described. The Grashof number measures the influence of thermal buoyancy on a fluid relative to its viscous force. As Gr changes, it enhances the buoyancy force while weakening the viscous forces. As the thickness of the fluid decreases, the internal resistance within the fluid also diminishes, causing the fluid to move faster.

Figures 6 and 7 explain how changes in the Modified Grashof Number (Gm) affect fluid movement. A higher Gm indicates that the buoyancy force is stronger compared to the force of viscosity. When the fluid's thickness decreases, its internal resistance decreases, allowing the fluid to move more swiftly.

The impact of the Hall effect on the primary and secondary velocities ( $u$ ,  $w$ ) can be observed in Figures 8 and 9. When the parameter  $m$  is increased in the boundary layer, the primary velocity ( $u$ ) decreases while the secondary velocity ( $w$ ) increases across the entire boundary layer area. This indicates

that the Hall current accelerates the movement of the secondary fluid within the boundary layer. This acceleration is due to the Hall current inducing a secondary flow in the fluid, which in turn slows down the movement of the primary fluid in the same area.

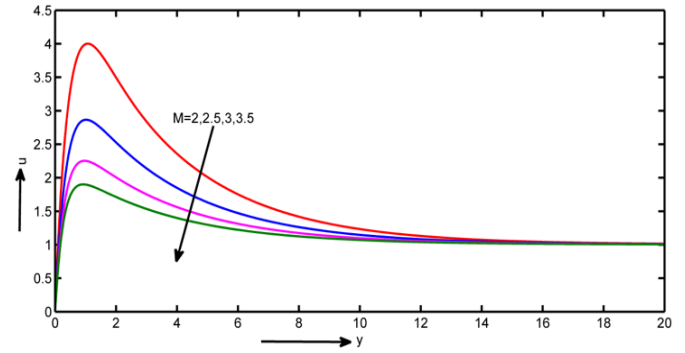


Figure 2. Influence of magnetic parameter on primary speed

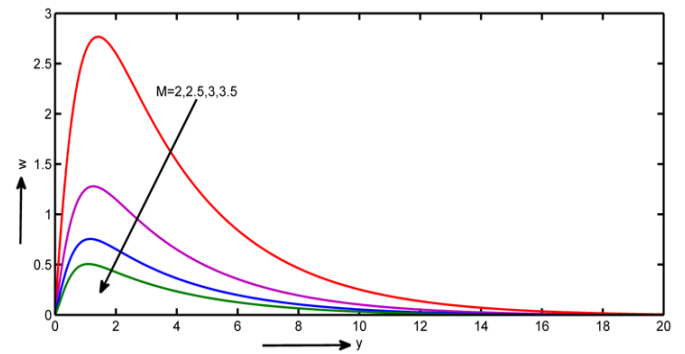


Figure 3. Influence of magnetic parameter on secondary speed

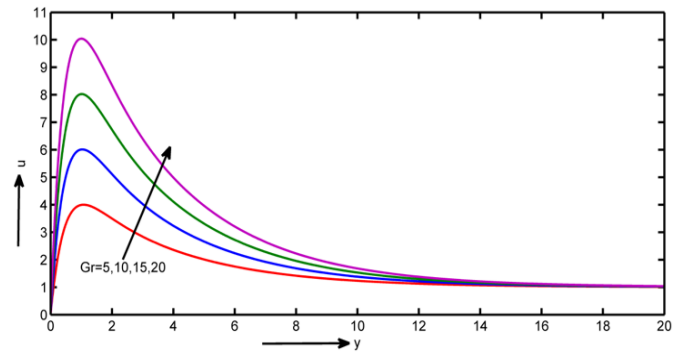


Figure 4. Influence of Grashof number on primary speed

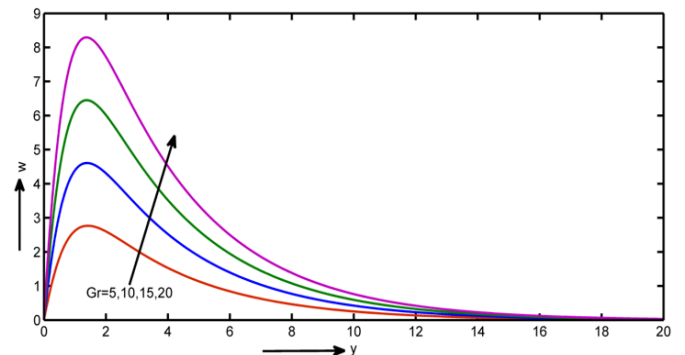
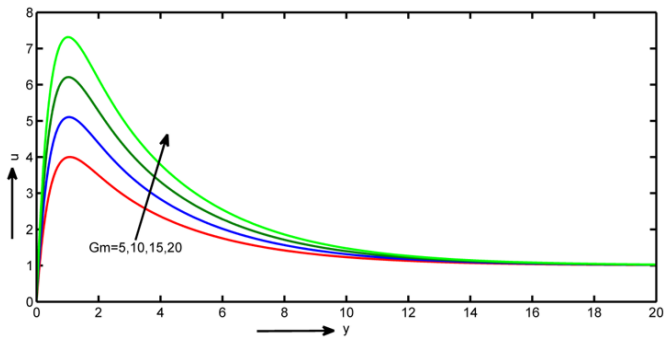
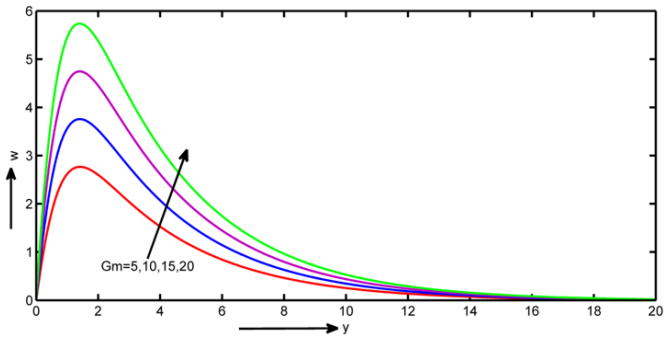


Figure 5. Influence of Grashof number on secondary velocity



**Figure 6.** Impact of modified Grashof number on primary velocity



**Figure 7.** Influence of modified Grashof number on secondary velocity

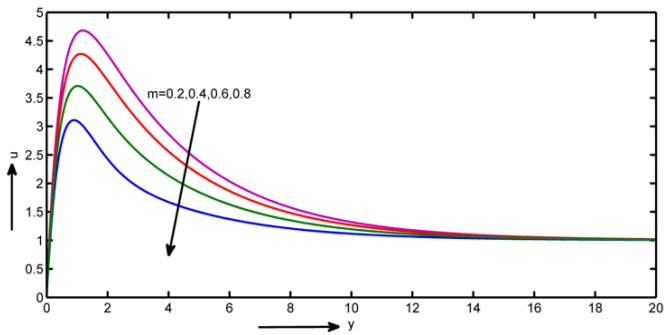


**Figure 8.** Influence of hall parameter on primary velocity

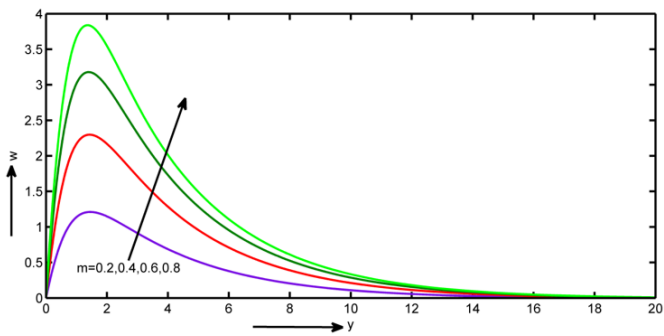


**Figure 9.** Influence of hall restriction on secondary rapidity

In Figures 10 and 11, velocity profiles are displayed, showing variations with the Dufour number ( $Du$ ). These figures indicate that the velocity increases as the Dufour parameter increases.

In Figures 12 and 13, velocity profiles are displayed with variations in radiation absorption ( $Ra$ ). These figures show

that the velocity increases as radiation absorption increases.

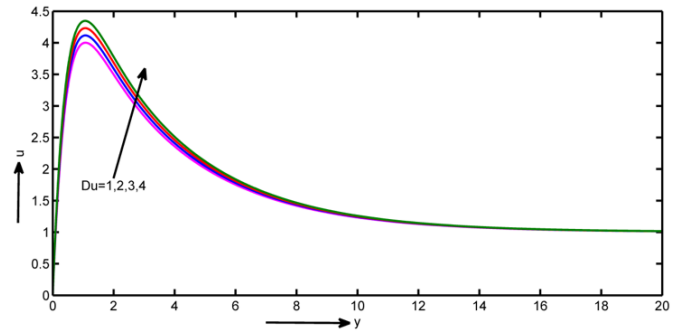


**Figure 10.** Impact of Dufour restriction on primary speed

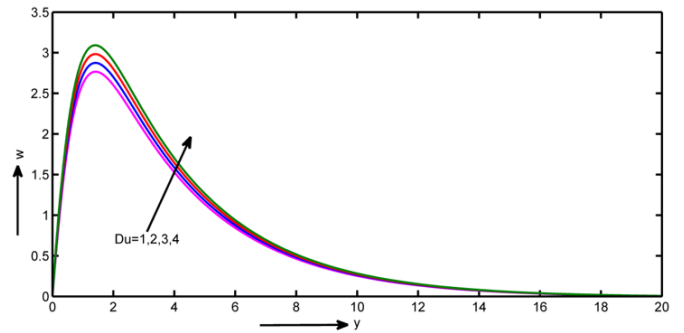


**Figure 11.** Influence of Dufour constraint on secondary speed

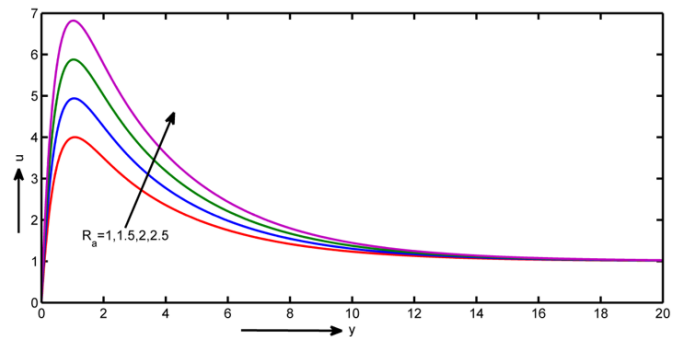


**Figure 12.** Effect of radiation absorption parameter on primary speed

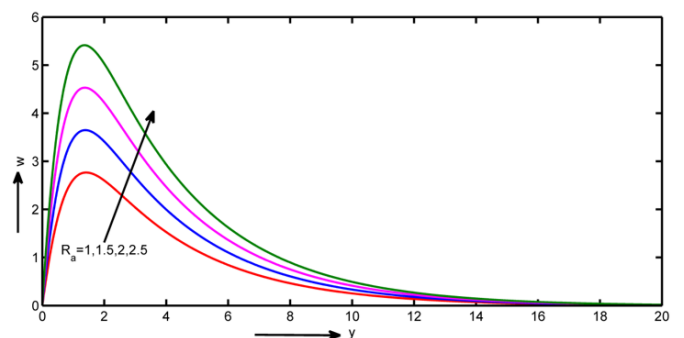


**Figure 13.** Impact of radiation absorption parameter on secondary speed

#### 4.2 Temperature profiles

Figures 14 to 18 illustrate the effects of various parameters such as Prandtl number ( $Pr$ ), radiation parameter ( $R$ ), heat



source parameter (Q), radiation absorption (Ra), and Dufour number (Du) on temperature distribution, respectively.

Figure 14 shows how the Prandtl number, denoted as "Pr," affects temperature profiles. The Prandtl number measures the ease with which heat moves through a fluid compared to how easily the fluid flows. A higher Prandtl number can slow the rate at which heat spreads. When thermal diffusivity decreases, it indicates that a material is less effective at conducting heat relative to its capacity to store heat, leading to lower temperature profiles.

Figure 15 demonstrates that higher values of the radiation parameter "R" increase the temperature profiles. Higher emission values enhance heat transport on the surface, thereby increasing the fluid's temperature.

Figure 16 illustrates the impact of varying levels of heat source parameter "Q" on temperature. As Q increases, the temperature within the field decreases. The data show that an increase in Q thins the thermal boundary layer and evens out the heat distribution across the layer. Additionally, the heat source acts to lower the fluid's temperature.

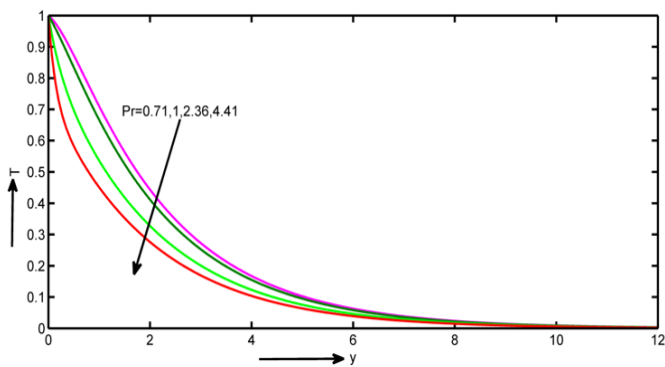


Figure 14. Impact of Prandtl number on temperature

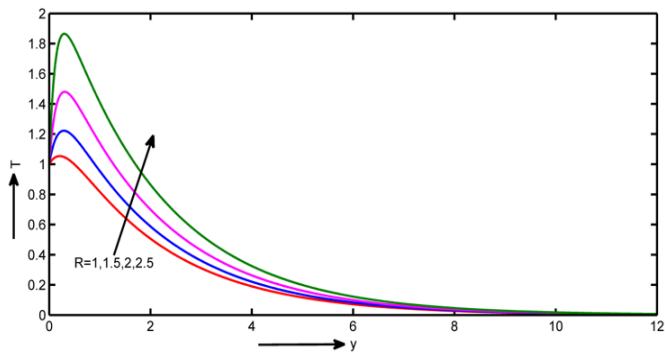


Figure 15. Radiation limitation's impact on temperature

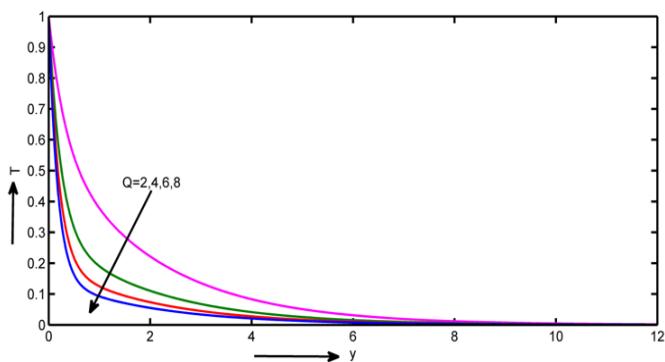


Figure 16. Heat source limitation's impact on temperature

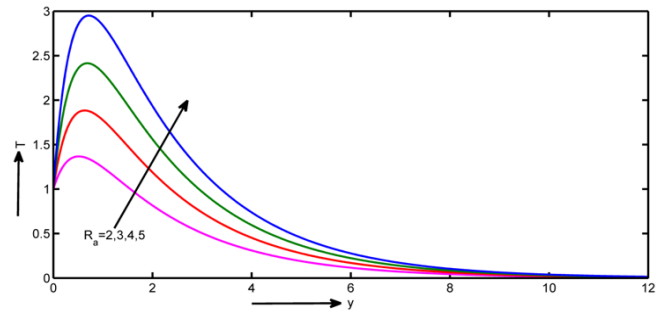


Figure 17. Temperature dependence of emission absorption limitation

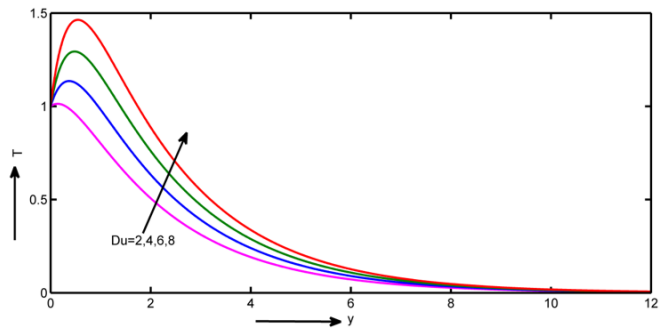


Figure 18. Dufour parameter's impact on temperature

The thickness of the thermal boundary layer near a surface increase with greater radiation absorption. When the radiation absorption parameter "Ra" is high, both the buoyant force and the thickness of the thermal boundary layers increase. This occurs because there is more heat transfer by conduction than absorption.

Figure 18 shows how the Dufour number (Du) affects temperature profiles. The Dufour effect occurs when heat flows due to a concentration gradient. When the Dufour effect is present, temperature profiles are higher than when it is absent. The flow near the boundary intensifies as the Dufour number increases, causing the thermal layer near the boundary to thicken due to Dufour effects.

### 4.3 Concentration profiles

The way the Schmidt number (Sc) affects the attentiveness curves is shown in Figure 19. The Schmidt number Sc shows how much momentum there is compared to how fast diffusivity spreads mass. It measures how well momentum and mass move through a boundary layer using diffusion in the hydrodynamic (velocity) and concentration (species) areas. An enlarge in the Schmidt number will lower the liquid's ability to diffuse mass resulting in a decrease in concentration profiles.

Figure 20 illustrates how the chemical reaction factor impacts the concentration profiles. This review examines the results of a harmful substance response ( $Kr > 0$ ). As the substance response increases the concentration levels decrease. In simple terms a chemical reaction involves a lot of clashes that can lead to destructive outcomes. This basically increases the movement of large molecules and improves the process of transportation which then reduces the spread of fluid flow concentration.

Table 1 shows that skin-friction ( $\tau$ ) decreases with an increase in Prandtl number (Pr), heat source parameter (Q), Kr, Schmidt number (Sc), and magnetic parameter (M), while it

increases with radiation absorption (Ra) and the Dufour effect (Du).

Table 2 indicates that the rate of heat transport increases with rising values of Pr, Q, and  $\eta$ , and decreases with increases

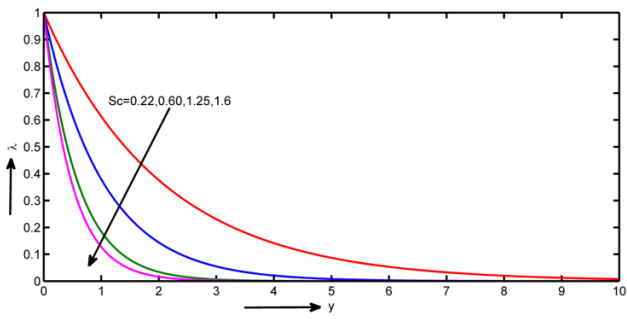


Figure 19. Influence of Schmidt number on concentration

in radiation absorption (Ra) and the Dufour effect (Du).

Table 3 observes that the rate of mass transfer increases when the values of the Schmidt number (Sc) and  $\xi$  are increased.

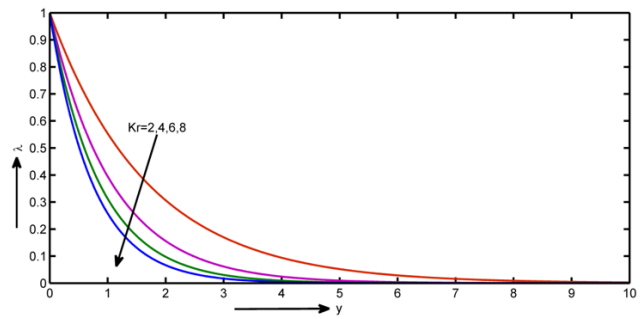


Figure 20. Influence of chemical reaction constraint on attentiveness

Table 1. Skin friction

Pr	Q	Kr	Sc	M	Du	Ra	Results of Obulesu [37] $\tau$	$\tau$ (present)
0.3							5.3187	5.3156
0.5							5.2844	5.2112
0.71							5.2481	5.1201
	1.5						5.1007	4.9987
	2						5.0617	4.9422
	2.5						5.0285	4.9136
		0.2					5.1337	5.0828
		0.4					5.1128	5.0282
		0.6					5.0969	4.9866
		0.8					5.0838	4.9522
			0.2				5.2483	5.1358
			0.3				5.2475	5.1003
			0.6				5.2469	4.9956
				0.5			5.6120	5.5841
				1			5.4818	5.4884
				1.5			5.3269	5.2487
				2			5.2203	5.1281
					2		...	5.3323
					4		...	5.5445
					6		...	5.7567
						1	...	6.9469
						3	...	10.3881
						5	...	13.8293

Table 2. Rate of heat transfer

Pr	Q	R	Ra	Du	Results of Obulesu [37] Nu	Nu (present)
0.1					1.2759	1.2797
0.5					1.5006	1.5755
0.71					1.6309	1.4566
7					7.2173	7.6218
	2				1.9764	1.9014
	3				2.2602	2.2893
	4				2.5068	2.5094
	5				2.7279	2.7926
		0.5			1.6309	1.6566
		0.6			1.6695	1.6784
		0.7			1.7071	1.7042
		0.8			1.7436	1.7343
			1		...	-0.4566
			3		...	-5.9269
			5		...	-11.3971
				2	...	-0.6254
				3	...	-0.7941
				4	...	-0.9629

Table 3. Rate of mass transfer

Sc	$\xi$	Results of Obulesu [37] Sh	Sh (present)
0.2		0.0347	0.0730
0.3		0.0823	0.0888
0.4		0.1321	0.1824
	0.1	0.0440	0.0544
	0.4	0.1123	0.1163
	0.6	0.1861	0.1896

## 5. CONCLUSIONS

When the Grashof number modified Grashof number Radiation absorption constraint and Dufour restriction go up the primary and secondary velocities also enhance.

The speed of the main and secondary flows reduces when the attractive restriction raises and the Hall effect is strengthened near the boundary layer. This causes the major pour speed to decrease as well as the secondary pour speed to have a overturn outcome on the main pour speed in the border

line sheet area.

Hotness reduces through an enlarge in Prandtl number, heat absorption constraint with rising through enhances at emission (R), radiation absorption restriction (Ra) and Dufour effect.

Concentration decreases with arising the values of Schmidt number, substance response.

When the heat absorption substance reaction Schmidt number Prandtl number and attractive constraint increase the skin friction reduces significantly. Moreover, while the emission amalgamation restriction (Ra) and Dufour effect values go up the skin friction coefficient also goes up.

The rate of heat transport raises with an add to Prandtl number, heat amalgamation restriction, emission restriction as well as also reverse effect from radiation absorption parameter (Ra) and Dufour effect.

The rate of mass transport raises with an amplify Schmidt number, substance response limitation.

## REFERENCES

- [1] Kumar, M.A., Reddy, Y.D., Goud, B.S., Rao, V.S. (2021). Effects of solet, DuFour, hall current and rotation on MHD natural convective heat and mass transfer flow past an accelerated vertical plate through a porous medium. *International Journal of Thermofluids*, 9: 100061. <https://doi.org/10.1016/j.ijft.2020.100061>
- [2] Kumaresan, E., Kumar, A.V. (2017). An exact solution on unsteady MHD viscoelastic fluid flow past an infinite vertical plate in the presence of thermal radiation. *Frontiers in Heat and Mass Transfer*, 8: 9. <https://doi.org/10.5098/hmt.8.9>
- [3] Jain, S., Choudhary, R. (2018). Soret and Dufour Effects on thermophoretic MHD flow and heat transfer over a non-linear stretching sheet with chemical reaction. *International Journal of Applied and Computational Mathematics*, 4(1): 50. <https://doi.org/10.1007/s40819-018-0481-2>
- [4] Gangadhar, K., Kannan, T., Jayalakshmi, P. (2017). Magneto hydrodynamic micropolar nanofluid past a permeable stretching/shrinking sheet with Newtonian heating. *Journal of the Brazilian Society of Mechanical Sciences and Engineering*, 39(11): 4379-4391. <https://doi.org/10.1007/s40430-017-0765-1>
- [5] Chu, Y.M., Alzahrani, F., Mopuri, O., Ganteda, C., Khan, M.I., Khan, S.U., Eldin, S.M. (2023). Thermal impact of hybrid nanofluid due to inclined oscillatory porous surface with thermo-diffusion features. *Case Studies in Thermal Engineering*, 42: 102695. <https://doi.org/10.1016/j.csite.2023.102695>
- [6] Prabhakar Reddy, B., Sademaki, L.J. (2022). A Numerical study on Newtonian heating effect on heat absorbing MHD Casson flow of dissipative fluid past an oscillating vertical porous plate. *International Journal of Mathematics and Mathematical Sciences*, 2022(1): 7987315. <https://doi.org/10.1155/2022/7987315>
- [7] Kabir, M.A., Al Mahbub, M.A. (2012). Effects of thermophoresis on unsteady MHD free convective heat and mass transfer along an inclined porous plate with heat generation in presence of magnetic field. *Open Journal of Fluid Dynamics*, 2(4): 120-129. <https://doi.org/10.4236/ojfd.2012.24012>
- [8] Sinha, S., Mahanta, M. (2019). Thermal diffusion (Soret Effect) on an unsteady MHD mixed convective heat and mass transfer flow through vertical porous medium with chemical reaction. *Science and Technology Journal*, 7(1): 69-77. <http://doi.org/10.22232/stj.2019.07.01.09>
- [9] Gangadhar, K., Kannan, T., Jayalakshmi, P., Sakthivel, G. (2021). Dual solutions for MHD Casson fluid over a shrinking sheet with Newtonian heating. *International Journal of Ambient Energy*, 42(3): 331-339. <https://doi.org/10.1080/01430750.2018.1550018>
- [10] Subhakar, M.J., Gangadhar, K., Reddy, N.B. (2012). Soret and Dufour effects on MHD convective flow of heat and mass transfer over a moving non-isothermal vertical plate with heat generation/absorption. *Advances in Applied Science Research*, 3(5): 3165-3184.
- [11] Sandhya, A., Reddy, G.R., Deekshitulu, G.V.S.R. (2019). Steady on MHD heat and mass transfer flow of an inclined porous plate in the presence of radiation and chemical reaction. *Journal of Physics: Conference Series*, 1344(1): 012002. <https://doi.org/10.1088/1742-6596/1344/1/012002>
- [12] Das, M., Mahanta, G., Shaw, S. (2020). Heat and mass transfer effect on an unsteady MHD radiative chemically reactive Casson fluid over a stretching sheet in porous medium. *Heat Transfer*, 49(8): 4350-4369. <https://doi.org/10.1002/htj.21830>
- [13] Nihaal, K.M., Mahabaleshwar, U.S., Joo, S.W., Lorenzini, G. (2023). Combined impact of joule heating, activation energy, and viscous dissipation on ternary nanofluid flow over three different geometries. *International Journal of Computational Methods and Experimental Measurements*, 11(4): 251-258. <https://doi.org/10.18280/ijcmem.110407>
- [14] Choudhury, K., Ahmed, N. (2018). Soret effect on transient MHD convective flow past a semi-infinite vertical porous plate with heat sink and chemical reaction. *Applications and Applied Mathematics: An International Journal (AAM)*, 13(2): 839-853.
- [15] Choudhury, R., Das, S.K. (2014). Visco-elastic MHD free convective flow through porous media in presence of radiation and chemical reaction with heat and mass transfer. *Journal of Applied Fluid Mechanics*, 7(4): 603-609.
- [16] Jayalakshmi, P., Gangadhar, K., Obulesu, M., Madhu Mohan Reddy, P. (2023). The axisymmetric flow of an MHD Powell-Eyring fluid with viscous dissipation and Newtonian heating condition: Keller-box method. *Heat Transfer*, 52(1): 936-948. <https://doi.org/10.1002/htj.22723>
- [17] Pothala, J., Mopuri, O., Ganteda, C., Peram, M.M.R., Kotha, G., Lorenzini, G. (2022). Effect of Newtonian heating on a magneto hydrodynamic boundary layer flow of a nanofluid over a stretching cylinder. *International Journal of Design & Nature and Ecodynamics*, 17(4): 481-489. <https://doi.org/10.18280/ijdne.170401>
- [18] Jayalakshmi, P., Obulesu, M., Ganteda, C.K., Raju, M.C., Varma, S.V., Lorenzini, G. (2023). Heat transfer analysis of Sisko fluid flow over a stretching sheet in a conducting field with Newtonian heating and constant heat flux. *Energies*, 16(7): 3183. <https://doi.org/10.3390/en16073183>
- [19] Khan, A.A., Zaimi, K., Sufahani, S.F., Ferdows, M. (2020). MHD flow and heat transfer of double stratified micropolar fluid over a vertical permeable shrinking/stretching sheet with chemical reaction and heat source. *Journal of Advanced Research in Applied*



- Sciences and Engineering Technology, 21(1): 1-14. <https://doi.org/10.37934/araset.21.1.114>
- [20] Dagana, J., Amos, E. (2020). MHD free convection heat and mass transfer flow in a porous medium with Dufour and chemical reaction effects. *International Journal of Innovative Scientific & Engineering Technologies Research*, 8: 1-12.
- [21] Podder, C., Samad, M.A. (2016). Dufour and Soret effects on MHD forced convective heat and mass transfer flow of Non-Newtonian power law fluid with thermal radiation and viscous dissipation. *American Journal of Applied Mathematics*, 4(6): 296-309. <https://doi.org/10.11648/j.ajam.20160406.16>
- [22] Srinivasacharya, D., Reddy, S.G. (2013). Soret and Dufour effects on mixed convection from a vertical plate in power-law fluid saturated porous medium. *Theoretical and Applied Mechanics*, 40(4): 525-542. <https://doi.org/10.2298/TAM1304525S>
- [23] Jha, B.K., Sarki, M.N. (2020). Chemical reaction and Dufour effects on nonlinear free convection heat and mass transfer flow near a vertical moving porous plate. *Heat Transfer*, 49(2): 984-999. <https://doi.org/10.1002/htj.21649>
- [24] Bordoloi, R., Ahmed, N. (2021). MHD free convection from a semi-infinite vertical porous plate with diffusion-thermo effect. *Biointerface Research in Applied Chemistry*, 12(6): 7685-7696. <https://doi.org/10.33263/BRIAC126.76857696>
- [25] Ahmed, N., Choudhury, K. (2019). Heat and mass transfer in three-dimensional flow through a porous medium with periodic permeability. *Heat Transfer-Asian Research*, 48(2): 644-662. <https://doi.org/10.1002/htj.21399>
- [26] Mopuri, O., Madhu, R.K., Peram, M.R., Ganteda, C., Lorenzini, G., Sidik, N.A. (2022). Unsteady MHD on convective flow of a Newtonian fluid past an inclined plate in presence of chemical reaction with radiation absorption and Dufour effects. *CFD Letters*, 14(7): 62-76. <https://doi.org/10.37934/cfdl.14.7.6276>
- [27] Taid, B.K., Ahmed, N. (2022). MHD free convection flow across an inclined porous plate in the presence of heat source, Soret effect, and chemical reaction affected by viscous dissipation Ohmic heating. *Biointerface Research in Applied Chemistry*, 12(5): 6280-6296. <https://doi.org/10.33263/BRIAC125.62806296>
- [28] Arulmozhi, S., Sukkiramathi, K., Santra, S.S., Edwan, R., Fernandez-Gamiz, U., Noeiaghdam, S. (2022). Heat and mass transfer analysis of radiative and chemical reactive effects on MHD nanofluid over an infinite moving vertical plate. *Results in Engineering*, 14: 100394. <https://doi.org/10.1016/j.rineng.2022.100394>
- [29] Umamaheswar, M., Reddy, P.C., Reddy, S.H., Mopuri, O., Ganteda, C.K. (2022). Aspects of parabolic motion of MHD fluid flow past a vertical porous plate with cross-diffusion effects. *Heat Transfer*, 51(5): 4451-4465. <https://doi.org/10.1002/htj.22507>
- [30] VeeraKrishna, M., Subba Reddy, G., Chamkha, A.J. (2018). Hall effects on unsteady MHD oscillatory free convective flow of second grade fluid through porous medium between two vertical plates. *Physics of Fluids*, 30(2): 023106. <https://doi.org/10.1063/1.5010863>
- [31] Obulesu, M., Raghunath, K., Sivaprasad, R. (2020). Hall current effects on MHD convective flow past a porous plate with thermal radiation, chemical reaction with radiation absorption. *AIP Conference Proceedings*, 2246(1): 020003. AIP Publishing. <https://doi.org/10.1063/5.0014423>
- [32] VeeraKrishna, M., Chamkha, A.J. (2018). Hall effects on unsteady MHD flow of second grade fluid through porous medium with ramped wall temperature and ramped surface concentration. *Physics of Fluids*, 30(5): 053101. <https://doi.org/10.1063/1.5025542>
- [33] Khlaf, A.M., Ehyaei, M.A., Abdul Wahhab, H.A. (2023). CFD simulation of premixed flame in counter burner under the influence of a magnetic field. *International Journal of Computational Methods and Experimental Measurements*, 11(4): 233-238. <https://doi.org/10.18280/ijcmem.110404>
- [34] Narayana, P.S., Venkateswarlu, B., Venkataramana, S. (2013). Effects of Hall current and radiation absorption on MHD micropolar fluid in a rotating system. *Ain Shams Engineering Journal*, 4(4): 843-854. <https://doi.org/10.1016/j.asej.2013.02.002>
- [35] Masthanrao, S., Balamurugan, K.S., K Varma, S.V., C Raju, V.C. (2013). Chemical reaction and hall effects on MHD convective flow along an infinite vertical porous plate with variable suction and heat absorption. *Applications and Applied Mathematics: An International Journal*, 8(1): 268-288.
- [36] Venkateswarlu, M., Makinde, O.D., Reddy, P.R. (2019). Influence of Hall current and thermal diffusion on radiative hydromagnetic flow of a rotating fluid in presence of heat absorption. *Journal of Nanofluids*, 8(4): 756-766. <https://doi.org/10.1166/jon.2019.1638>
- [37] Obulesu, M., Prasad, R.S. (2020). Hall current effects on MHD convective flow past a porous plate with thermal radiation, chemical reaction with thermophoresis. *Annals of the Faculty of Engineering Hunedoara*, 18(3): 205-212.
- [38] Deebani, W., Tassaddiq, A., Shah, Z., Dawar, A., Ali, F. (2020). Hall effect on radiative Casson fluid flow with chemical reaction on a rotating cone through entropy optimization. *Entropy*, 22(4): 480. <https://doi.org/10.3390/e22040480>
- [39] Mishra, A., Sharma, B.K. (2017). MHD mixed convection flow in a rotating channel in the presence of an inclined magnetic field with the Hall effect. *Journal of Engineering Physics and Thermophysics*, 90: 1488-1499. <https://doi.org/10.1007/s10891-017-1710-y>
- [40] Deka, R.K. (2008). Hall effects on MHD flow past an accelerated plate. *Theoretical and Applied Mechanics*, 35(4): 333-346. <https://doi.org/10.2298/TAM0804333D>
- [41] Srinivasacharya, D., Jagadeeshwar, P. (2017). MHD flow with Hall current and Joule heating effects over an exponentially stretching sheet. *Nonlinear Engineering*, 6(2): 101-114. <https://doi.org/10.1515/nleng-2016-0035>

## NOMENCLATURE

$C$	The fluid's species concentration; $K.mol. m^{-3}$
$C_{\infty}$	Concentration of species in the fluid distant from the plate; $K.mol. m^{-3}$
$C_w$	Fluid species concentration close to the plate; $K.mol$
$C_p$	Temperature at constant pressure; $J.Kg^{-1}.K^{-1}$
$D_M$	Diffusion of molecules in chemicals; $m^{-2}.s^{-1}$
$\rho$	Density of the substance; $Kg.m^{-3}$
$g$	Gravitational acceleration; $m.s^{-2}$

$q_r$	Radiative heat flux; $W.m^{-2}$
$T$	Temperature of the fluid; K
$T_\infty$	Temperature outside of the plate's range; K
$T_w$	The plate's temperature; K
$t$	Time
$u^*$	A speed component along x - axis; $m.s^{-1}$
$v^*$	A speed component along y - axis; $m.s^{-1}$
$v$	Velocity of the fluid; $m.s^{-1}$
$v_0$	Scale of the suction velocity; $m.s^{-1}$
$M$	Magnetic field parameter
$m$	Hall parameter
$Du$	Dufour number
	Radiation parameter
$Q$	Heat absorption parameter
$R_a$	Radiation absorption parameter
$Pr$	Prandtl number
$Gr$	Thermal Grashof number
$Gm$	Modified Grashof number
$Kr$	Chemical reaction parameter

### Greek symbols

$\mu$	Coefficient of viscosity; $Kg.m^{-1}.s^{-1}$
$\kappa$	Temperature sensitivity; $W.m^{-1}.K^{-1}$
$\sigma$	Conductivity of electricity; $\frac{1}{\Omega.m}$
$\vartheta$	Motion viscosity; $m^2.s^{-1}$
$\beta$	Coefficient of volume expansion; $J.kg^{-1}.K^{-1}$

### APPENDIX

$$\eta_1 = (1 + R)Q$$

$$\delta_1 = (1 + R) \left( Q + \frac{i\omega Pr}{4} \right)$$

$$\alpha_1 = \frac{M^2}{1 + m^2} (1 - im)$$

$$\alpha_2 = \alpha_1 + \frac{1}{K_1}$$

$$\alpha_3 = \alpha_1 + \frac{i\omega}{4} + \frac{1}{K_1}$$

$$A_1 = \frac{Sc + \sqrt{Sc^2 + 4Sc\xi}}{2}$$

$$A_2 = \frac{Sc + \sqrt{Sc^2 + 4Sc(\xi + \frac{i\omega}{4})}}{2}$$

$$A_3 = \frac{Pr + \sqrt{Pr^2 + 4\eta_1}}{2(1 + \eta)}$$

$$A_4 = \frac{Pr + \sqrt{Pr^2 + 4\delta_1}}{2(1 + \eta)}$$

$$A_5 = \frac{1 + \sqrt{1 + 4\alpha_2}}{2}$$

$$A_6 = \frac{1 + \sqrt{1 + 4\alpha_3}}{2}$$

$$a_1 = A_1^2 - ScA_1 - Sc(\xi + \frac{i\omega}{4})$$

$$a_2 = (1 + R)A_1^2 - PrA_1 - Qa_3 = (1 + R)A_3^2 - PrA_3 - (Q + \frac{i\omega Pr}{4})$$

$$a_4 = (1 + R)A_2^2 - PrA_2 - \left( Q + \frac{i\omega Pr}{4} \right) a_5$$

$$= (1 + R)A_1^2 - PrA_1 - \left( Q + \frac{i\omega Pr}{4} \right)$$

$$a_6 = A_1^2 - A_1 - \alpha_2 a_7 = A_3^2 - A_3 - \alpha_2$$

$$a_8 = A_1^2 - A_1 - \alpha_3 a_9 = A_2^2 - A_2 - \alpha_3$$

$$a_{10} = A_3^2 - A_3 - \alpha_3 a_{11} = A_4^2 - A_4 - \alpha_3$$

$$a_{12} = A_5^2 - A_5 - \alpha_3 l_2 = \frac{DuA_1^2 + R_a}{a_2}$$

$$l_1 = 1 + l_2 l_3 = PrA_3$$

$$l_1 l_4 = \frac{DuScA_1 A_2^2 + R_a ScA_1}{a_1}$$

$$l_5 = \frac{a_1 PrA_1 l_2 + DuScA_1^3 + R_a ScA_1}{a_1}$$

$$l_6 = \frac{l_3}{a_3} l_7 = \frac{l_4}{a_4} l_8 = \frac{l_5}{a_5}$$

$$l_9 = l_8 - l_7 - l_6$$

$$l_{10} = \frac{Gr l_1}{a_7}$$

$$l_{11} = \frac{Gm - Gr l_2}{a_6}$$

$$l_{12} = 1 - l_{10} - l_{11}$$

$$B_1 = \frac{Gm Sc A_1}{a_1}$$

$$l_{13} = \frac{A_1 l_{11} + B_1 - Gr l_8}{a_8}$$

$$l_{14} = \frac{Gr l_7 - B_1}{a_9}$$

$$l_{15} = \frac{A_3 l_{10} + l_6 Gr}{a_{10}}$$

$$l_{16} = \frac{a_{11}}{Gr l_9}$$

$$l_{17} = \frac{A_5 l_{12}}{a_{12}}$$

$$l_{18} = 1 - (l_{13} + l_{14} + l_{15} + l_{16} + l_{17})$$